Total Sytem Error Performance During Precision Approaches

Robert Geister
German Aerospace Center
Institute of Flight Guidance
Braunschweig, Germany

Thomas Dautermann
German Aerospace Center
Institute of Flight Guidance
Braunschweig, Germany

Michael Felux
German Aerospace Center
Institute of Communication and Navigation
Oberpfaffenhofen, Germany

***Abstract*—This paper gives an overview of the error performance of different navigation sensors used in an A320 research aircraft. In particular, the Total System Error (TSE) performance during precision approaches is investigated. Different approaches based on the Instrument Landing System (ILS) as well as based on the GNNS Landing System (GLS) were conducted manually with a research aircraft of the German Aerospace Center (DLR). The main focus of the work is put on comparing the TSE during the two different types of approaches. The goal is to show that the TSE performance is equivalent for both guidance systems and that GLS could therefore be used for simultaneous approach operations onto parallel runways. In addition, the position accuracy in the vertical domain of different sensors is investigated. Here we compare a Ground Based Augmentation System (GBAS) and the barometric altitude sensor of the basic aircraft.**

Keywords-GBAS; ILS; Total System Error Performance; VNAV

I. INTRODUCTION

Since the 1940s the traditional form of guidance of aircraft on final approach was provided by the Instrument Landing System (ILS). It consists of two transmitters which provide guidance in the horizontal and vertical planes. A localizer, situated behind the runway end to which approach service is provided, gives lateral guidance on the approach and during roll out on the runway [1]. For vertical guidance a glide slope transmitter is placed next to the runway abeam the touchdown point at a safe distance [2]. Both systems transmit narrow beams with different modulations: slightly left and right to the extended centerline for the localizer; and slightly above and below the desired glide path for the glide slope. This enables the aircraft to determine its instant deviation from the predefined approach track. However, the fixed antenna installation can only provide one single straight reference path and does not support optimized curved approach tracks in terms of noise abatement or reduced fuel consumption.

Since the introduction of Global Navigation Satellite Systems (GNSS) in the 1990s, the aviation community has been very interested in its further use for this purpose. The ICAO identified GNSS as one of the main enablers for progress in Air Traffic Management (ATM) with the potential to greatly increase capacity of airspace systems [3]. Despite its great nominal performance, however, standalone GPS is not able to provide sufficient accuracy and integrity for approach and landing operations. The imaginable impact of several potential sources for significant positioning errors, including ionospheric disturbances (see [4], [5] and [6]) Radio Frequency Interference (RFI) and several others requires additional techniques or systems that can provide a means to detect errors or provide corrections, together with integrity information. Receiver Autonomous Integrity Monitoring is a technique in which redundant GNSS measurements are used to check plausibility of the navigation solution and to identify potentially faulty satellites or associated measurements. This method can guarantee a certain level of integrity and in combination with inertial navigation supports operations with Required Navigation Performance (RNP). However, it only monitors and does not correct any potential errors. Corrections for GNSS measurements are, for example, provided by Space Based Augmentation Systems (SBAS) such as the US Wide Area Augmentation System (WAAS) and the European Geostationary Navigation Overlay Service (EGNOS). Both operate a wide area network of ground stations which monitor the GNSS satellites and ionospheric conditions and provide this information to users via geostationary satellites. A user is thus able to correct for a great part of the ionospheric disturbance and place a significant amount of trust in the correctness of navigation signals. WAAS is capable of providing lateral and vertical approach guidance down to a decision height of 200ft and EGNOS to a minimum decision height of 250ft (see [7], [8]).

However, not all error effects can be detected and reflected in the transmitted parameters within the required time to alarm in order to support aircraft instrument approaches with a lower or no decision height and automatic landings. With current satellite navigation systems this can only be achieved by means of a Ground Based Augmentation System (GBAS). A GBAS, or Local Area Augmentation System (LAAS) as it is referred to in the US, consists of typically four reference receivers which are located at the airport to which approach service is provided. They generate locally relevant differential GNSS corrections and provide integrity parameters which allow arriving aircraft to navigate with the required level of accuracy and integrity. Since the system is installed at the airport, the achievable time to alarm is much shorter than for SBAS. Currently, systems

supporting CAT-I operations (i.e., instrument guidance to a decision height of not less than 200ft, visual continuation afterwards) are certified and the first stations became operational (Bremen, Newark, Houston) or are in the process of obtaining approval (Malaga, Zürich). The standards for GBAS supporting CAT-II/III operations are currently undergoing validation and are expected to be fully adopted by ICAO in 2018 [9].

The introduction of the GNSS Landing System (GLS) in addition to ILS poses several new questions in terms of operations, especially regarding mixed operations at airports operating both systems simultaneously. This will likely become the nominal situation for the foreseeable future as ILS will not be decommissioned for many years. Especially for parallel approaches one needs to take a detailed look at the difference in performance of both systems in order to ensure that simultaneous approaches based on different systems do not pose any safety risks. Currently, ILS and MLS are the only guidance systems which can be used for simultaneous parallel approach operations [10]. GLS could be used as another guidance system for such parallel approach operations provided that approaching aircraft using GLS follow the desired flight path like they would in the ILS case. In addition, some research is currently ongoing to investigate whether GLS could even enable segmented parallel approaches to use the runway capacity more efficiently [11]. Below, the Total System Error (TSE) performance of GLS operations is compared to the performance of ILS before the decision height (visual part of an instrument approach starts afterwards). The analysis is based on flight data which was collected during several approaches with an Airbus A320 research aircraft to the airport of Braunschweig, Germany (cf. Table I). Braunschweig airport is equipped with both an ILS and a GBAS ground station. Similar GLS flight trials were performed in [12] with smaller aircraft. In this work a single transport category aircraft is used for ILS and GLS approaches.

Different components exist, that add up to the TSE, i.e. the total displacement from the ideal approach path. The error that is made in defining the flight path (resolution limits of digital data systems) is called Path Definition Error (PDE). It is usually negligible and is not considered in this study. The error between the actual aircraft position and the estimated position from the navigation system is called the Navigation System Error (NSE). Finally, the difference between the estimated flight path and the defined flight path is called Flight Technical Error (FTE). This part of the TSE is attributed to the pilot or autopilot and the capability to follow a predefined path. All those errors are illustrated in Figure 1. They are usually divided into their lateral and the vertical components. In this paper, we show the NSE performance of ILS and GBAS as well as the FTE and the resulting TSE.

The purpose of this study is to obtain an initial estimate whether the TSE during GLS approaches is comparable to the TSE of the well-established ILS approaches. Presently, simultaneous operations onto a parallel runway system are only allowed when using ILS for the approach.

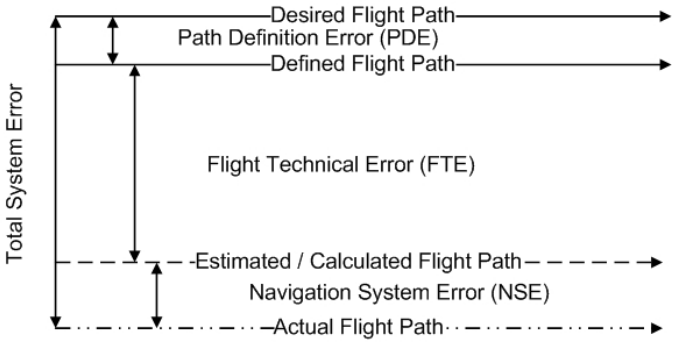

Figure 1: Flight Path Error Types

II. METHODS

A. Setup of experimental hardware

The presented data were gathered during different flights with the A320 research aircraft of the German Aerospace Center, the Advanced Technology Research Aircraft (ATRA). The aircraft is equipped with a basic flight test instrumentation that records data from the different sensors and systems of the basic (unmodified) aircraft. This includes data from the barometric altitude system, aircraft attitude data and ILS receiver deviations. Additional experimental equipment was integrated for these flight trials. First, an experimental cockpit display was integrated on the right side of the cockpit. On this display, a Primary Flight Display (PFD), a Navigation Display (ND) and an Engine Display (ED) were shown (see Figure 2). Secondly, two racks were integrated in the cabin. In these racks, a Septentrio GNSS receiver was used to gather GNSS data. The Septentrio receiver is capable of receiving and recording raw GNSS and raw SBAS data.

The Septentrio data were used for post processing of a carrier phase solution after each flight which serves as the true reference position. The data were used and processed in the same way as within an avionics grade GBAS receiver according to the specifications in [13] and [14].


Figure 2: ATRA experimental cockpit display

The GNSS receivers were connected to an experimental antenna on top of the fuselage. The sensors for the barometric altimetry system are located on the lower fuselage. The antennas for the ILS system are located at the nose of the aircraft (see Figure 3).

B. Flight Trial Setup

The results from the flight trials conducted with ATRA were all obtained during manual flight with a flight director shown to the pilot on the experimental cockpit display (see Figure 2). The approaches shown here were either ILS or GLS approaches. They were all conducted at Braunschweig-Wolfsburg airport (ICAO: EDVE) and flown onto both runway ends (26 and 08).

The flight trials were performed over a period of two years. During this time, the runway at the airport was extended and the Glide Path Angle (GPA) of the ILS system was changed from 3.5° to 3.0°. The GLS approaches were designed to be an exact copy of the ILS approach and were verified as such [15]. As both GPAs are permitted by ICAO for an ILS Category I (CAT I) approaches, flight trials with both GPAs are considered in this work and it is not differentiated between them in the analysis.

From an operational point of view, the approaches were conducted in a similar fashion. During both types of approaches, the aircraft was intercepting the localizer with a certain offset (usually 30°) and afterwards the glideslope was intercepted. However, some of the GLS approaches considered here had a curved leg at the beginning of the approach. These legs were neglected here to compare only straight in ILS and "ILS-look-alike" approaches.

The data presented were obtained from the flights shown in TABLE I. In total, six ILS approaches as well as eight GLS approaches were evaluated, all manually flown, following a flight director bar on the experimental display.

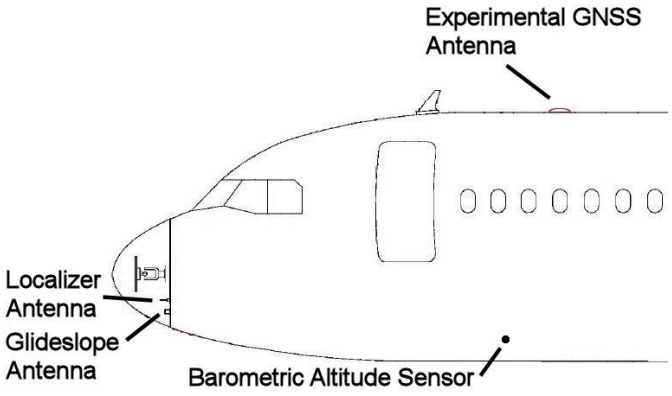

Figure 3: Approximate antenna and sensor positions

In order to classify the NSE during the flights, the Dilution of Precision (DOP) was considered. The DOP is an indication of how well the aircraft's position can be estimated by GNSS as a result from the prevailing satellite geometry. TABLE II. shows the minimum and maximum values of the Horizontal and Vertical DOP during each flight. The DOP values were used as quality indicators of the calculated NSE. It can be seen that the DOP values are small enough to use the calculated NSE in our investigations. The values are shown for the entire flight and not only for the conducted approaches.

TABLE I. DATES OF FLIGHT TRAILS

Flight No. #	Dates of Flights		
	Date	*No. of ILS Appr.*	*No. of GLS Appr.*
1	10/06/2011	3	0
2	10/06/2011	1	1
3	01/23/2013	0	3
4	09/19/2013	2	4

TABLE II. DILUTION OF PRECISION DURING TRIALS

Flight No. #	Table Column Head			
	Max VDOP	*Min VDOP*	*Max HDOP*	*Min HDOP*
1	1.88	1.10	1.29	0.89
2	1.65	1.0	0.97	0.75
3	1.68	0.95	1.09	0.76
4	2.97	1.23	1.06	0.68

C. Data reduction

The results for the ILS approaches were derived from the localizer and glideslope deviations that were recorded directly from the onboard ILS receiver in Differences in Depth of Modulation (DDM). Both ILS localizer and glide path transmitter broadcast two narrow radio beams from the same antenna array: for the localizer one slightly to the left of the centerline, one slightly to the right, for the glide path one slightly above and one slightly below the desired descent path. The two lobes are modulated with 90 and 150Hz, respectively. DDM measures the difference of the modulation strength between those two beams which can be transformed into an angular deviation and displayed to the pilot. The recorded DDM values were transformed to degrees with the formula given in [14]

$$\alpha_{lat,\,degrees} = \frac{\text{Lat.Deviation}_{DDM}}{0.155} \times \tan^{-1}\left(\frac{Course\ Width\ at\ Threshold}{Dist\ Threshold\ to\ Azim.\ Ref.\ Point}\right) \quad (1)$$

and the assumption that a full scale deflection occurs at 0.155 DDM. Reference [14] describes the local area augmentation system, but, as the GLS approaches were designed to be equal to the ILS approach, the calculations yield comparable results. These angular deviations recorded from the ILS and GLS systems represent the FTE during the approaches. In the same manner the vertical FTE was transformed with:

$$\alpha_{vert,\,degrees} = \text{Vertical Deviation}_{DDM} \times \left(\frac{0.25\ x\ GPA}{0.175}\right) \quad (2)$$

The results for the GLS approaches presented in this work are based on data recorded with a Septentrio PolaRx3 receiver onboard the aircraft. This Septentrio receiver is not GBAS capable by itself, but the data gathered from this receiver was

used together with the GBAS messages received by a Multi-Mode Receiver to calculate a GBAS solution after the flight. The software used to do so was the PEGASUS toolset provided by EUROCONTROL [16].

Besides the signal on the GPS L1 frequency (1.57542 GHz), the Septentrio PolarRx3 is also capable of recording the encrypted military signal on the GPS L2 frequency (1.2276 GHz) using a semi-codeless tracking algorithm. Using this second frequency, errors induced by the ionosphere can be eliminated. Moreover, this high end receiver also tracks and records the carrier phase of the signal received on both frequencies with three decimals. One phase cycle corresponds to about 19cm on GPS L1 and 24 cm on L2. However, it is not known to the receiver, how many integer cycles are present on the signal at the time when initial lock is established. Therefore, the recorded carrier phase signal has one integer ambiguity for each receiver satellite pair. In post-processing, these ambiguities can be resolved and the carrier phase measurement can be used for positioning. In case a reference station with dual frequency data and a precisely known position is located in the area of interest, the resolution process becomes faster and more precise. Furthermore, congruent errors between this reference and the rover can be eliminated in a manner similar to GBAS. For further details please refer to [21],[22] or other textbooks on GNSS positioning.

To determine the true position of the aircraft, dual frequency carrier phase data from the Septentrio receiver was post-processed with RtkLib 4.2.2 [17] relative to the IGS reference site PTBB [18] located at the Physikalisch Technische Bundesanstalt (PTB) about 6km southwest of the airport. The reference solution was obtained using kinematic integer ambiguity resolution, which yields sub decimeter RMS accuracy [19].

This position reference was used to determine the deviations from the desired flight path according to [14]. This is equivalent to the way that deviations are calculated by the MMR and the Pegasus toolset. Additionally, the GLS approach is designed to be equal to the ILS approach and therefore all deviations are comparable. The deviations from desired flight path were calculated using the true reference position. These deviations represent the TSE for each flight. For every flight the TSE and the FTE were obtained in post-processing. The NSE was calculated by subtraction of the FTE from the TSE. In summary the following data was used:

- TSE; deviations from the desired path calculated based on the reference position according to [14], corrected for the different antenna positions
- FTE; deviations from the desired path received by the onboard ILS and for GBAS obtained by the Pegasus toolset based on the calculated GBAS position of the Septentrio receiver
- NSE=TSE - FTE

All data were time synchronized using GPS time stamps. To compare the different approaches to each other, all data was presented in terms of distance to the runway threshold. The distance to the runway threshold was calculated based on the reference position.

For the approaches, deviations were considered if the aircraft was established on the final approach path (laterally and vertically) and the system was operational. In addition, data was only considered until a go-around was initiated. As stated above, some of the GLS approaches had a curved leg at the beginning. Therefore, the final approach path was significantly shorter (approx. 5000m) than the ILS final approach. This can be seen in the results we present in this work.

Furthermore, for the determination of the vertical NSE (and therefore the TSE) all position data was corrected for the different locations of the antennas and sensors. All positions were transformed to the GNSS antenna position of the Septentrio PolaRx3 (as shown in Figure 3). Therefore, the glideslope signals and the signals from the barometric altimetry system were corrected taking the attitude of the aircraft into account. With these corrected results, the vertical position of the different systems (GBAS and barometric altimeter) was compared. In this case data was considered throughout the flight if the respective system was operational (e.g. the aircraft was within GBAS coverage region).

III. RESULTS

The flight trial data were synchronized and sorted with regard to the distance to the runway threshold. This was done based on the reference position obtained in post-processing.

A. *Results for ILS*

Figure 4 shows the mean TSE and plusminus one standard deviation over the distance to the runway threshold during all six investigated ILS approaches. The red line indicates the lateral TSE and the green line indicates the vertical TSE. The standard deviation for every mean value is shown as error bars.

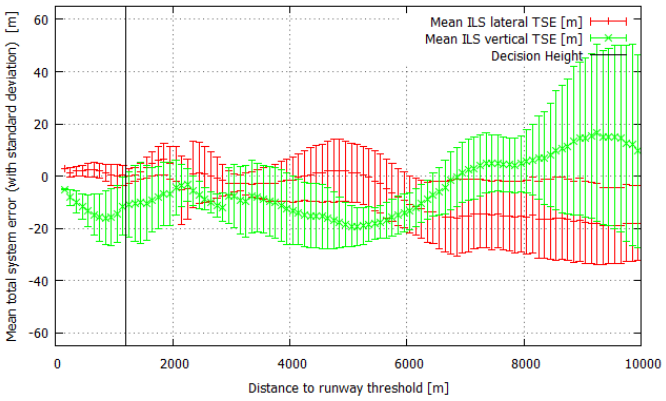

Figure 4: ILS Mean TSE

Figure 5 shows an example of the recorded ILS FTE during three approaches. The red crosses represent the localizer deviation in degrees over the distance to the runway threshold. The deviations are transformed from DDM to degrees according to formula (1) as given above. The green crosses indicate the glideslope deviations over the distance to the runway threshold. It can be seen that especially the localizer signal is distorted to a certain degree further away from the

threshold. It has to be stated that the vertical deviation indication is more sensitive than the lateral deviation indication as the full scale deflection occurs sooner in the vertical case (at 0.75° for a 3° glide slope according to formula (2)) than in the lateral case (approx.. 2.2° in our investigated setup). Therefore, it is possible to steer the aircraft more precisely in the vertical domain than in the lateral. The figure below shows however that the values for the lateral and vertical deviations are very similar.

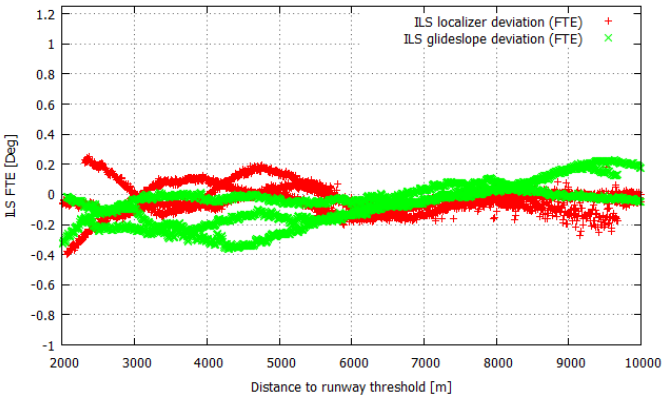

Figure 5: ILS Devs FTE example

B. *Results for GLS*

For the GLS approaches, data was only considered if the aircraft was on a straight final. In some of the flights curved approaches were investigated. As the curved part is not comparable to ILS, data gathered before the straight final segment of those approaches were disregarded. Figure 6 shows an example of the GLS FTE during three GLS approaches.

It can be seen that the deviations are a lot smoother and steadier than in the ILS case. Here, the red crosses indicate the lateral GLS deviations in degrees over the distance to the runway. The green crosses indicate the vertical GLS deviation. The magenta crosses indicate a curved approach during which the pilot was not able to intercept the straight final approach segment promptly. This approach was not considered in the analysis of the lateral errors but is shown here for reference it can also be seen that the curved leg ended around 7000m away from the runway threshold (excluding the magenta line with close-in curve). Therefore, only lateral deviations observed beyond that point were considered in the analysis presented here.

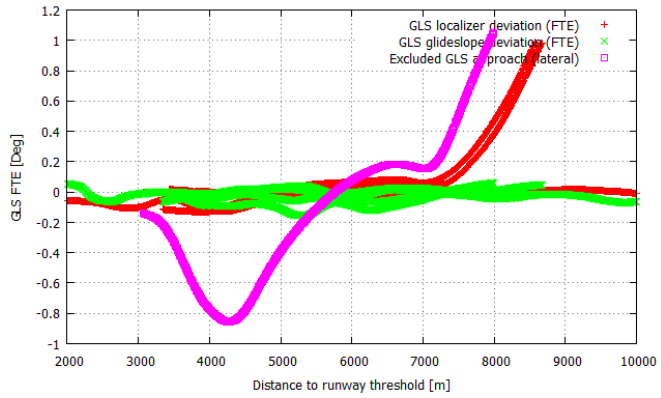

Figure 6: GLS Devs FTE example

Figure 7 shows the mean lateral TSE for seven considered GLS approaches from a distance of 7400m from the runway threshold. The error bars indicate again one standard deviation around every mean value. The triangles indicate the number of data points associated with each bin.

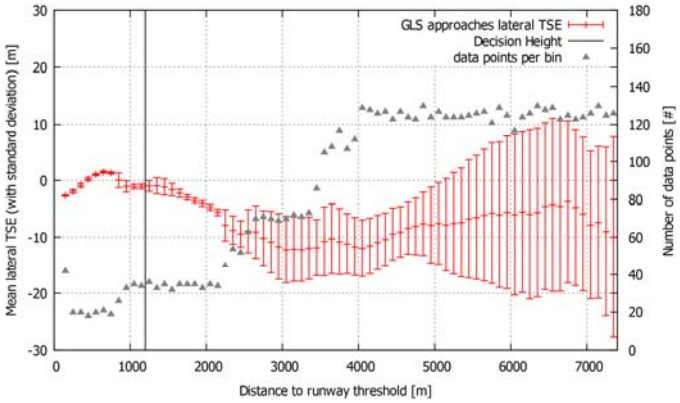

Figure 7: Mean lateral TSE during GLS approaches

Figure 8 shows the same data for the vertical TSE during GLS approaches. Here, eight approaches were considered. In both figures the standard deviation decreases towards the runway threshold as fewer approaches were continued to perform a landing and less data was available as shown by the triangles. Many of the approaches were discontinued between 1000m and 2000m from the threshold by a go-around in order to conduct more approaches in a single flight.

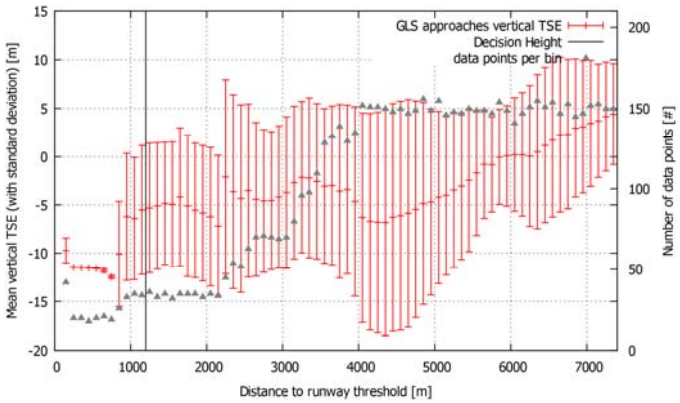

Figure 8: Mean vertical TSE during GLS approaches

As described above, one of the components of the TSE is the FTE. Figure 9 shows the mean lateral FTE (green) and NSE (blue) of the seven approaches considered. Figure 10 shows the mean FTE (green) and NSE (blue) for the vertical domain. All eight approaches are considered again. Comparing the NSE and the FTE it becomes evident that the FTE is the major component of the TSE during a GLS approach. It was found that the vertical TSE is increasing significantly after the decision height during the visual part of the approach (see Figure 10 at distances smaller than 1200m).

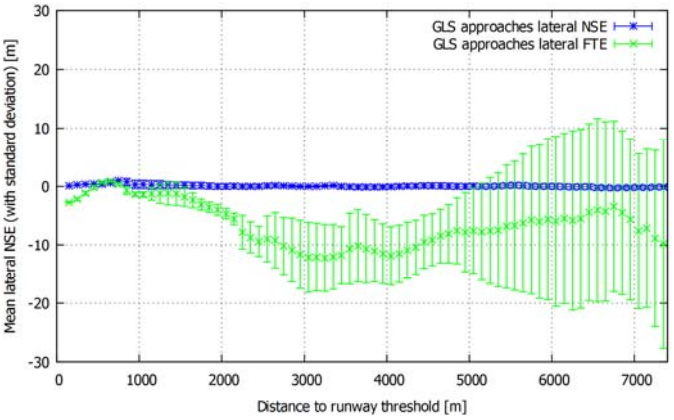

Figure 9: Mean lateral FTE and NSE during GLS approaches

The second investigated component of the TSE is the NSE. The NSE of GBAS was gathered by subtracting the observed FTE from the calculated TSE in order to account for the along-track error. Figure 11 shows the mean lateral NSE during the final straight segment of the seven considered GLS approaches. It can be seen that the error is generally small and distributed around zero.

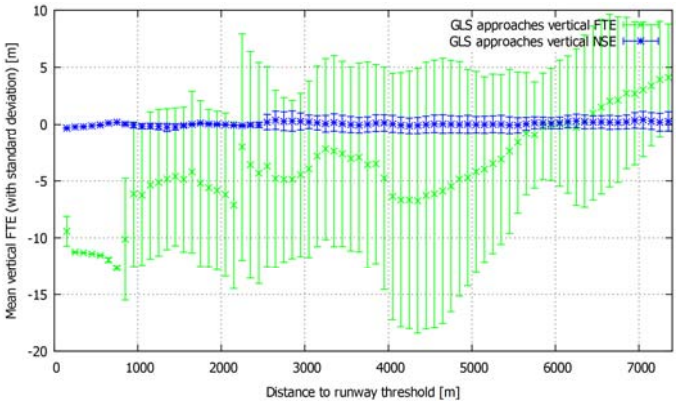

Figure 10: Mean vertical FTE and NSE during GLS approaches

Figure 12 shows the mean vertical NSE of the eight considered GLS approaches. The vertical NSE is as well generally small and distributed around zero.

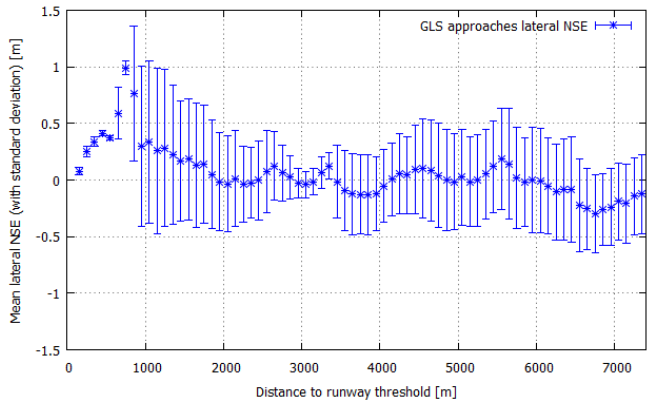

Figure 11: Mean lateral NSE during GLS approaches

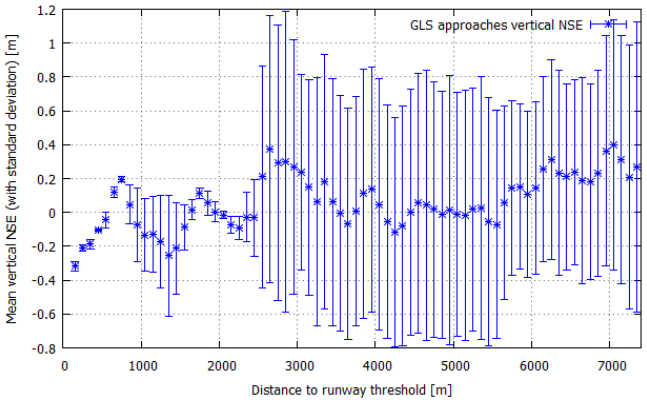

Figure 12: Mean vertical NSE during GLS approaches

In order to compare the vertical NSE performance from different sources in the GBAS coverage region, the error distribution during that period of a single flight is shown in Figure 13. The green histogram shows the NSE distribution for GBAS. The blue one shows the vertical NSE distribution of the barometric altimetry system.

As stated above, data was only taken into account if the aircraft was established on the localizer and the glide slope and before a go around was initiated and before the decision height. As multiple approaches were flown during one flight and only a single final landing was conducted, the usable data close to the runway threshold are sparse due to the small number of approaches. Therefore, care should be taken in analyzing the data statistically.

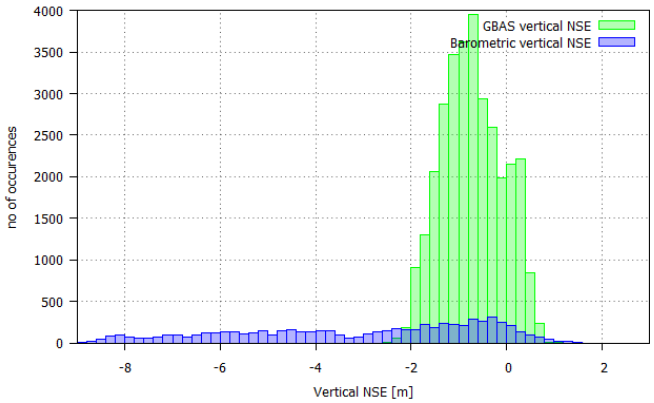

Figure 13: NSE distribution during the approaches of a single flight (GBAS, green and barometric altitude, blue)

IV. Discussion

For GLS approaches, it is evident that the lateral NSE is fairly small (the mean error remains generally smaller than 0.5m in the analyzed flight trials) compared to the FTE. It has to be stated, that some of the conducted GLS approaches had a curved leg. The capture of the straight final approach segment is therefore somewhat more difficult and it occurred slightly later than for standard straight-in approaches. This is visible in Figure 6 (magenta points) between approximately 3500m and 5000m away from the threshold. Especially during this approach the pilot was not able to intercept the localizer

promptly after a curved leg. Therefore this approach was not considered in the analysis of the lateral error performance.

The vertical NSE for GLS approaches is also rather small and shown to be of similar magnitude as the lateral NSE. The observed TSE (both laterally and vertically) is well within the assumed reference values of the ILS collision risk model [20] which indicates a standard deviation for the lateral TSE of 22.4m at 1200m away from the runway threshold in the given setup, for example. Furthermore, it indicates a standard deviation for the vertical TSE of approximately 7m at 1200m away from the runway threshold and a glide path angle of 3.5°.

To be able to compare the ILS TSE and the GLS TSE, the analysis focused on the last part of the final approach in Figure 14. There, it is visible that the TSE of both types of approaches at this distance to the runway threshold (where ILS is the most accurate) is very similar and very small. This is especially notable when considering that the allowable lateral alert limit for the NSE of GLS approaches alone is approximately 40m at this distance to the threshold.

When comparing the vertical TSE (Figure 15), it can be seen that the observed error in the approaches is smaller during GLS approaches than during ILS approaches. As the curved approaches already had a glide path angle corresponding to the final segment, they do not have an influence on the vertical TSE in this case.

When investigating the vertical NSE of the barometric altimeter, it can be seen that the setting of the barometric correction of the pilot has a direct influence. If the local reference air pressure changes over time and the vertical pressure distribution is not the one used for altimeter calibration, the NSE will increase. This error will prevail until the pilot adapts the barometric correction setting. Therefore, the NSE is not normally distributed and usually greater than for GBAS.

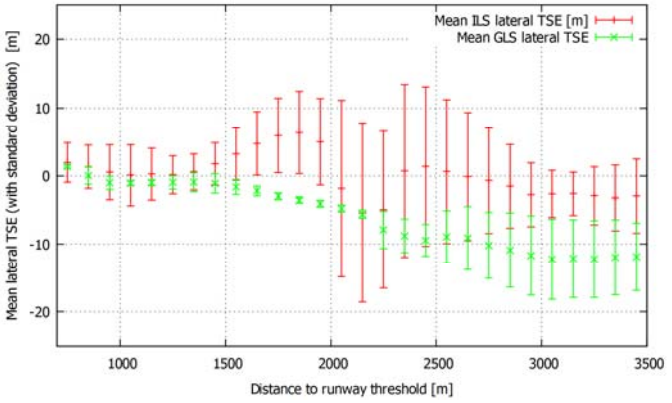

Figure 14: Comparison of mean lateral TSE during ILS (red) and GLS (green) approaches

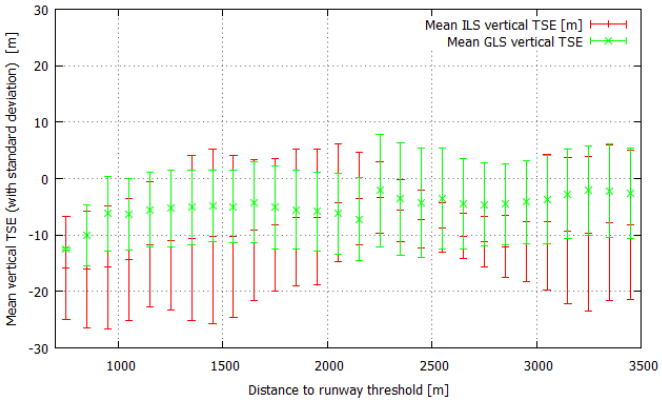

Figure 15: Comparison of mean vertical TSE during ILS (red) and GLS (green) approaches

V. CONCLUSION

GLS TSE performance is similar to the ILS TSE performance and would therefore allow the same type of simultaneous operations onto parallel runways. As the results presented here are based on a small number of approaches, the analysis must be verified with additional data to be statistically relevant. When verification of small probabilities is required, a significant number of approaches must be analyzed to obtain meaningful results. A ballpark number for this would be to obtain at least ten times more data than the inverse probability under investigation (i.e. for a probability of 10^{-6} perform at least 10 million flights, for a probability of 0.05 at least 200 flights). Especially for small probabilities, this task is often difficult or not at all achievable and computer simulations must be run. In general the stochastic Law of Large Numbers applies, which states that after sufficiently large number of empirical trials, the empirical error distribution will approximate the underlying distribution.

The results show that the largest part of the TSE is the FTE portion. GLS NSE performance is significantly better than ILS NSE performance. Our investigations thus indicate that the design concept of GLS being introduced as “ILS-look-alike” yields comparable behavior.

The flight trial data shown here indicate that the GLS TSE is in the same range as during ILS approaches, and therefore GLS could be used for simultaneous operation into a parallel runway system.

In addition, the vertical position accuracy for GBAS is higher and more reliable than the barometric vertical position accuracy and effort should be made to introduce augmented satellite systems as the main source of the vertical position information rather than barometric altimetry systems.

ACKNOWLEDGMENT

The authors would like to thank the DLR flight department as well as the involved air traffic controllers in Braunschweig and the surrounding airspace for the great cooperation throughout all the trials. In addition, the authors would like to thank the PEGASUS Team from EUROCONTROL for their quick and exhaustive support. We would also like to thank

Patrick Rémi from the DLR Institute for Communication and Navigation for his support during the data processing.

REFERENCES

[1] RTCA, “RTCA DO-195 - Minimum operational performance standards for airborne ILS localizer receiving equipment operating within the radio frequency range of 108-112 MHz”, RTCA, 1986, Washington, D.C., USA

[2] RTCA, “RTCA DO-192 - Minimum operational performance standards for airborne ILS glide slope receiving equipment operating within the radio frequency range of 328.6-335.4 MHz”, RTCA, 1986, Washington, D.C., USA

[3] ICAO, “Doc 9849 - Global navigation satellite system (GNSS) manual”, first edition, ICAO, 2005, Montréal, Canada

[4] C. Mayer, B. Belabbas, N. Jakowski, M. Meurer, W. Dunkel, “Ionosphere threat space model assessment for GBAS”, proceedings of the ION ITM, 2009, Anaheim, CA, USA

[5] S. Pullen, YS Park, P. Enge, “The impact and mitigation of ionosphere anomalies on ground-based augmenation of GNSS”, proceedings of the 12th International Ionospheric Effects Symposium, 2008, Alexandria VA, USA

[6] T. Murphy, M. Harris, “Mitigation of the ionospheric gradient threats for GBAS to support CATII/III”, proceedings of the ION GNSS, 2006, Forth Worth, TX, USA

[7] T. Dautermann, “Civil air navigation using GNSS enhanced by wide area satellite based augmentation systems”, Progress in Aerospace Science, 2014, in press

[8] ICAO, “Doc 8168-OPS/611 - Procedures for Air Navigation Services Volumes 1 and 2”, ICAO, 2006, Montréal, Canada

[9] ICAO NSP WGW, “GBAS CAT II/III development baseline SARPs - draft proposed changes to Annex 10, Volume I”, ICAO, 2010, Montréal, Canada

[10] ICAO, “Doc 9643 - Manual on simultanious operations on parallel or near-parallel instrument runways (SOIR)”, first edition, ICAO, 2004, Montréal, Canada

[11] C. Hanses, “An initial safety concept for segmented independent parallel approaches”, proceedings of Integrated Communications Navigation and Surveillance Conference (ICNS), 2013, Washington, D.C., USA.

[12] L. Boniface, “The ILS equivalency methodology and GBAS flight test results - ICAO obstacle clearance panel”, working group meeting proceedings (WP35), 2002, Brussels, Belgium

[13] RTCA, “DO-246D - GNSS Based Precision Approach Local Area Augmentation System (LAAS) – Signal-in-Space Interface Control Document”, RTCA, Incorporated, 2008, Washington D.C. (USA)

[14] RTCA, “DO-253C - Minimum operational performance standards for gps local area augmentation system airborne equipment”, RTCA, Incorporated, 2008, Washington D.C., USA

[15] R. Geister, T. Ludwig, I. Jessen, “Installation and validation of a GBAS ground station at the research airport Braunschweig-Wolfsburg”, proceedings of CEAS 2009, 2009, Machester, UK

[16] EUROCONTROL, PEGASUS GNSS data analysis toolset, 2003, Brétigny-sur-Orge (France), https://www.eurocontrol.int/articles/pegasus

[17] RTKLIB: An Open Source Program Package for GNSS Positioning, http://www.rtklib.com/

[18] PTB reference station, IGS station ptbb, http://igscb.jpl.nasa.gov/network/site/ptbb.html

[19] T. Takasu, A. Yasuda, “Development of the low-cost RTK-GPS receiver with an open source program package RTKLIB”, proceedings of international symposium on GPS/GNSS, 2009, Jeju, Korea

[20] ICAO, “Doc 9274-AN/904 - Manual on the use of the collision risk model (CRM) for ILS operations”, first edition, ICAO, 1980, Montréal, Canada

[21] P. Misra, P. Enge “Global Positioning System: Signals, Measurements and Performance”, Second Edition, 2006, Ganga Jamuna Press, Lincoln, Massachusets, USA

[22] S. Gleason, D. Gebre-Egziabher, “GNSS Applications and Methods”, 2009, Artech House, Norwood, MA, USA